Origin of the Elastic Behavior of Syndiotactic Polypropylene

Finizia Auriemma, Odda Ruiz de Ballesteros, and Claudio De Rosa*

Dipartimento di Chimica, Università di Napoli "Federico II", Complesso Monte S.Angelo, Via Cintia, 80126 Napoli, Italy

Received November 28, 2000; Revised Manuscript Received March 22, 2001

ABSTRACT: An analysis of the mechanical properties and a detailed structural study of samples of syndiotactic polypropylene (sPP) are presented in order to clarify the origin of the elastic behavior of sPP. Samples of sPP having different stereoregularity and showing different polymorphic behavior have been analyzed. The present study allows to establish that the elastic properties of unoriented specimens of sPP are poor, since the initial dimensions are only partially recovered upon the release of the stress. Good elastic properties are, instead, shown by sPP fibers, which have been previously oriented (for instance, uniaxially drawn at 400% and at 600% their initial length and then stress-relaxed). Tension set values less than 10% are attained for these fibers. The elastic properties of sPP mainly originate from a reversible crystal−crystal phase transition which occurs during the stretching and when the tension is removed. The stable crystalline modification of sPP with chains in the helical conformation transforms into the crystalline form with chains in the *trans*-planar conformation (form III) by stretching. Upon release of the stress, the *trans*-planar form transforms again into the helical form. The recovery of the dimension of the fibers is associated with the reversible strain of the chain conformation and, hence, of the crystalline lattice. From this analysis it is possible to conclude that, while the driving force which induces the recovery of the initial dimensions in common elastomers upon the release of the stress is mainly entropic, in the case of sPP it is basically linked to the enthalpy gain achieved when the sample is relaxed, which involves a crystal−crystal phase transition from the metastable form III to the more stable helical modification (form II).

Introduction

Thermoplastic elastomers are generally poorly crystalline materials, with glass transition temperatures much below the room temperature, which partially crystallize under stretching.[1] Their elastic behavior is generally ascribed to two factors:

(1) The average chain dimensions (i.e., gyration radius, end-to-end distance) are modified by the external mechanical field, since the chains tend to assume rather elongated conformations with the chain axes preferentially oriented along the stretching direction. This conformational transition is reversible, since, upon the release of the stress, the initial set of conformations (globally identified with the term "random coils"), and hence the initial chain dimensions, are recovered on average.

(2) The small crystalline domains produced by the stretching act as physical cross-links, preventing the material from flowing and hence hindering almost completely plastic deformations. Upon release of the stress, the degree of crystallinity is reduced and the material recovers the initial dimensions.

The natural rubber and rigid−flexible polyesters and polyurethanes (as for instance Pibiflex and Lycra) are good examples of thermoplastic elastomeric materials showing the above-described behavior.

The first example of thermoplastic elastomeric polypropylene is that one isolated by Natta in the late 1950s[2−4] by fractionating polypropylenes made with conventional titanium- and vanadium-based catalysts. The elastic behavior of this material was interpreted in terms of a stereoblock microstructure of the chains, consisting of alternating blocks of amorphous atactic stereosequences and isotactic stereosequences which are able to crystallize and act as physical cross-links.

In recent years several authors have described new strategies for synthesizing elastomeric polypropylene, using different catalysts. Highly active catalysts consisting of metal oxide supporting Zr and Ti alkyls[5−7] produce a high molecular weight stereoblock polypropylene which, unlike the elastomeric polypropylene isolated by Natta,[2] does not require fractionation and exhibits good elastic properties as polymerized. Elastomeric polypropylenes can also be produced by different classes of metallocene-based catalysts: unbridged zirconocene catalysts[8,9] produce a reactor blend of stereoblock polypropylenes which can be separated in fractions of different tacticities and melting points, whereas asymmetric titanocenes[10] and zirconocenes[11,12] produce low melting or amorphous polypropylenes having a more homogeneous composition. Moreover, the C_2[13] and C_{2v}-symmetric[14] zirconocenes can produce poorly isotactic or high molecular weight atactic polypropylenes, respectively, showing good elastic properties.

Syndiotactic polypropylene (sPP) is a thermoplastic material showing elastic behavior which cannot be ascribed to the above-mentioned factors. It is, indeed, a high crystalline material with a relatively high glass transition temperature (−10 °C < T_g < 0 °C), whose elastic properties are associated with a reversible crystal−crystal polymorphic transition.[15,16] In fact, drawing procedures induce a crystal−crystal phase transition from the most stable crystalline modifications with chains in the 2-fold helical $(T_2G_2)_n$ conformation into the metastable form III with chains in the *trans*-planar conformation. This transition is almost completely reversible: the fibers transform again in the helical form upon the release of the tension,[16] and a partial, or even a nearly total, recovery of the initial dimensions of the sample is achieved.[17,18]

10.1021/ma002021j CCC: $20.00
Published on Web 05/25/2001

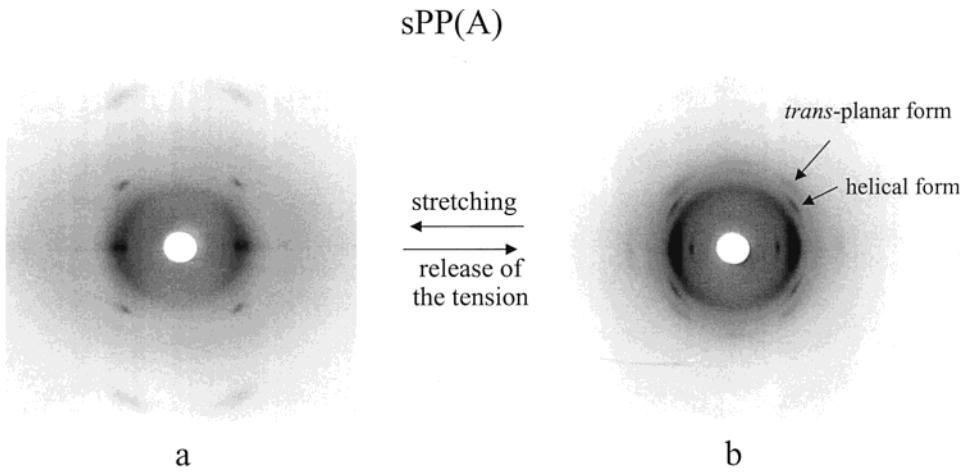

Figure 1. X-ray fiber diffraction patterns of oriented fibers of the sPP(A) sample, obtained by stretching compression-molded films at 400% elongation (nearly at break), kept in tension (a) and after the release of the tension after 2 days (b). The arrows indicate reflections on the first layer line arising from the diffraction of portions of crystals in the *trans*-planar form III with a periodicity of 5.1 Å and in the helical form II with a periodicity of 7.4 Å. The relative intensities of these reflections indicate that the fiber in (b) is basically in the helical form II. The fiber in (a) is in the pure *trans*-planar form III.

It is worth noting that a reversible crystal−crystal phase transition between stretched and relaxed states have been found also in polyethers[19,20] and in some aromatic polyesters.[21,22] In particular, in the case of the poly(trimethylene terephthalate) and poly(tetramethylene terephthalate) also a recovery from strain of the materials has been observed,[22] which has been associated with reversible strains of the crystalline lattices.[21]

In this paper the elastic behavior of sPP has been analyzed in order to give evidence that this property is strictly related to the reversible crystal−crystal phase transition involving a change in the conformation of the chains. A parallel analysis of the mechanical properties and the polymorphic behavior of various sPP samples having different stereoregularity is presented. Since a different stereoregularity induces a different polymorphic behavior in stretched samples of sPP,[16] different mechanical properties of these samples are expected. The comparison between the structural and the mechanical properties of these samples will allow to clarify the mechanism underlaying to the elastic behavior of sPP. A comparison with the elastic properties of a not vulcanized natural rubber sample is also presented.

Experimental Section

Three different samples of sPP were analyzed. Two samples (sPP(A) and sPP(B)), supplied by Montell Technology, were synthesized with a single center syndiospecific catalyst composed of isopropylidene(cyclopentadienyl)(9-fluorenyl)zirconium dichloride and methylaluminoxane.[23] sPP(A) ($M_w = 2.13 \times 10^5$, $M_w/M_n = 2.4$) and sPP(B) ($M_w = 1.93 \times 10^5$, $M_w/M_n = 4.5$) samples were prepared at different temperatures and are characterized by fully syndiotactic pentad contents [*rrrr*] of 93 and 78% and melting temperatures of 143 and 124 °C, respectively. The third sample, sPP(C), was synthesized with the traditional Ziegler−Natta vanadium-based catalyst[24] at very low temperature. The sample sPP(C) is stereoirregular and regioirregular, being characterized by a stereoblock structure with syndiotactic sequences prevailing in respect to isotactic ones, head-to-head/tail-to-tail regioirregular defects[25,26] and a melting temperature of nearly 120 °C. The sample of natural (not vulcanized) rubber examined here ($M_w = 81\,000$) was kindly furnished by Dr. M. Galimberti of Pirelli S.p.A. in Milan.

Compression-molded specimens (0.3 mm thick) were obtained by quenching from the melt to room temperature the sPP samples and to 0 °C the sample of natural rubber. X-ray powder diffraction patterns (not reported) indicate that all three examined sPP samples are crystallized in the most stable form I.[15]

The mechanical tests were performed at room temperature on a miniature mechanical tester apparatus (Minimat, by Rheometrics Scientific) following the standard test method for tensile properties of thin plastic sheeting ASTM D882-83. The mechanical tests were first performed on the unstretched compression-molded films. Rectangular specimens 10 mm long, 5 mm wide, and 0.3 mm thick were stretched up to a given strain. The mechanical tests were then performed also on the strained and stress-relaxed material; that is, the stretched films were kept under tension for 2 days, and then the tension was removed, allowing the specimens to relax. These stress-relaxed fibers were subjected to other strains. The free gauge length was 10 mm, and the ratio between the drawing rate and the initial length was fixed equal to 0.1 mm/(mm min), for the measurement of Young's modulus and 1 mm/(mm min) for the measurement of stress−strain curves and the determination of the other mechanical properties (stress and strain at break, tension set). The tension set values were measured according to the standard test method ASTM D412. The specimens with initial length L_0 were stretched up to a length L_f and held at this elongation for 2 days, then the tension was removed, and the final length of the relaxed specimens L_r was measured after 10 min. The tension set was calculated by using the following formula: $t_s = [(L_r - L_0)/L_0] \times 100$, whereas the elastic recovery was calculated as $r = [(L_f - L_r)/L_r] \times 100$. The reported values of the mechanical properties are averaged over at least five independent experiments.

The X-ray fiber diffraction patterns were obtained with Cu Kα radiation, monochromatized with a graphite single crystal, and recorded on a BAS-MS imaging plate (FUJIFILM) using a cylindrical camera and processed with a digital imaging reader (FUJIBAS 1800).

Results and Discussion

The X-ray fiber diffraction patterns of the oriented fibers of the sPP(A) and sPP(B) samples are reported in Figures 1 and 2, respectively. The patterns of the fibers obtained by stretching compression molded films at 400% elongation and holding the sample under tension are shown in part a of Figures 1 and 2, while the patterns obtained after the release of the tension are shown in part b of the same figures. It is apparent that for the most stereoregular sPP(A) sample the pure *trans*-planar form III is obtained by stretching (Figure 1a), as indicated by the presence of the equatorial

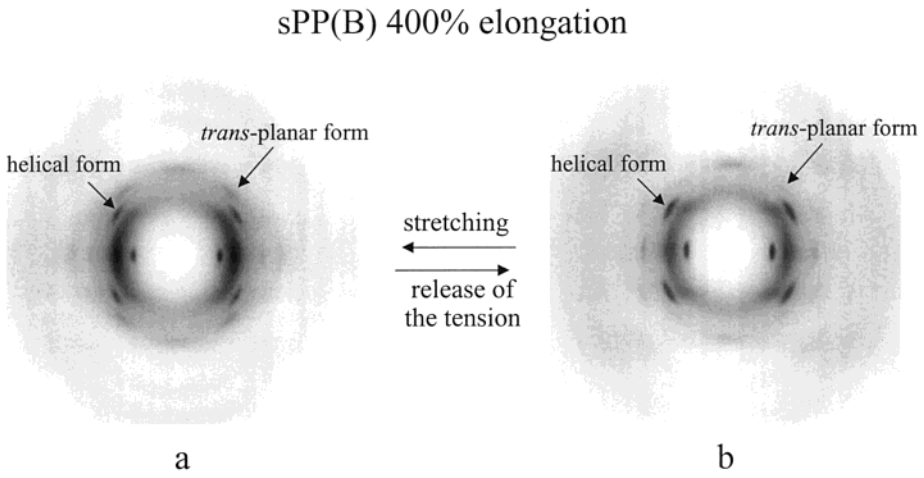

Figure 2. X-ray fiber diffraction patterns of oriented fibers of the sPP(B) sample, obtained by stretching compression-molded films at 400% elongation, kept in tension (a) and after the release of the tension after 2 days (b). The arrows indicate reflections on the first layer line arising from the diffraction of portions of crystals in the *trans*-planar form III with a periodicity of 5.1 Å and in the helical form with a periodicity of 7.4 Å. The relative intensities of these reflections indicate that the fiber in (a) is a mixture of the *trans*-planar form III and the helical form II, whereas the fiber in (b) is basically in the helical form II.

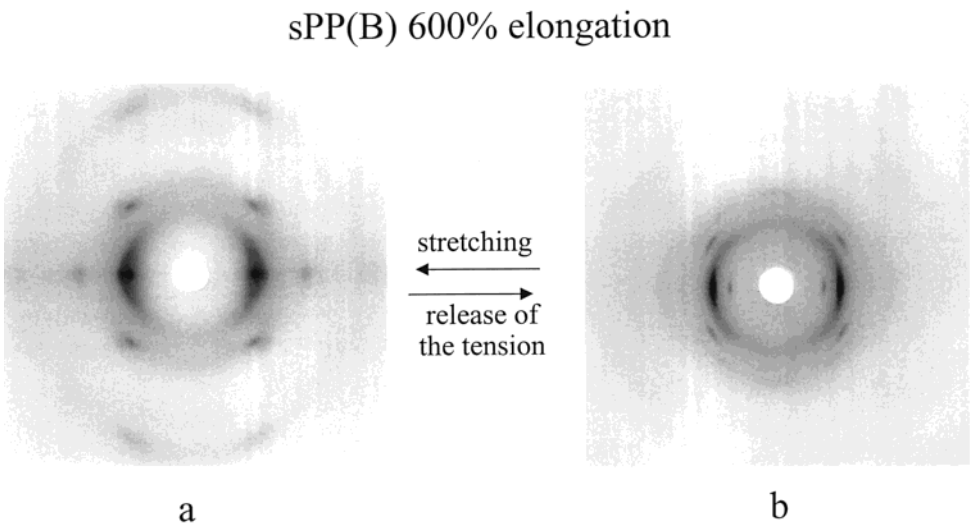

Figure 3. X-ray fiber diffraction patterns of oriented fibers of the sPP(B) sample, obtained by stretching compression-molded films at 600% elongation, kept in tension (a) and after the release of the tension after 2 days (b). The fiber in (a) is in the pure *trans*-planar form III, whereas the fiber in (b) is in the pure helical form II.

reflections at $d = 5.57$ and 4.72 Å ($2\theta = 15.9°$ and 18.8°, respectively), and spots on the first layer line corresponding to a chain periodicity of $c = 5.1$ Å.[27] For the less stereoregular sPP(B) sample a mixture of the *trans*-planar form III and the crystalline modification of sPP with chains in helical conformation is obtained by stretching (Figure 2a). This is clearly indicated by the presence of a strong equatorial reflection at $d = 7.2$ Å ($2\theta = 12.3°$), typical of the helical form of sPP, and spots on layer lines corresponding to both chain periodicities of $c = 5.4$ Å (*trans*-planar) and $c = 7.4$ Å (2-fold helical).[15]

From the pattern of Figure 2a, it is difficult to decide whether the crystalline portion of the material with chains in helical conformation is form I or form II or a mixture of both, since a large diffraction spot is present on the equator around $2\theta = 15°-19°$; in this 2θ region, indeed, the main diffraction peaks of form III as well as the most diagnostic peaks of form I and form II (occurring at $d = 5.6$ Å, $2\theta = 15.8°$ and $d = 5.22$ Å, $2\theta = 17.0°$, respectively)[15] strongly overlap. Most likely, this helical portion of the material is in form II since, according to literature data, uniaxial drawing procedures at room temperature produce the pure form II in poorly stereoregular sPP samples.[16]

It is worth noting that for higher draw ratios, of the order of at least 600%, the pure *trans*-planar form III is obtained also for the sPP(B) sample (Figure 3a), while for draw ratios higher than 400% the most stereoregular sPP(A) sample breaks.

After the release of the tension both sPP(A) and sPP-(B) samples remain partially oriented, while the *trans*-planar form III transforms into the helical fully isochiral form II, as indicated by the equatorial 200 and 110 reflections at $d = 7.2$ Å ($2\theta = 12.3°$) and $d = 5.22$ Å ($2\theta = 17.0°$), respectively, and the 111 reflection on the first layer line in the patterns of Figures 1b, 2b, and 3b. A small amount of crystals in form III is preserved in these fibers as indicated by the presence in Figures 1b and 2b of weak diffraction spots on the layer lines corresponding to the chain periodicity of $c = 5.1$ Å. The fiber in Figure 3b is, instead, in the pure form II as indicated by the absence of reflections of the *trans*-planar form III and the sharpness of the 110 reflection at $2\theta = 17.0°$.

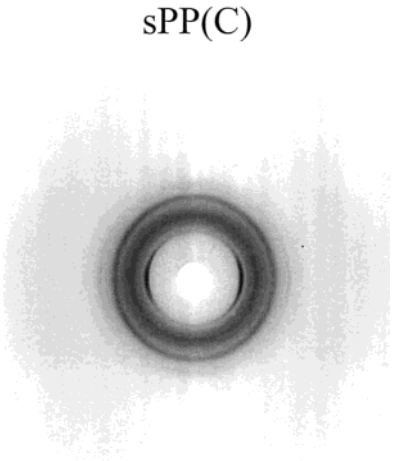

Figure 4. X-ray fiber diffraction pattern of the compression-molded sPP(C) sample stretched at 300% elongation (nearly at break) and kept in tension (helical form II).

This crystal−crystal transition is reversible; upon successive stress−relaxation cycles, form II transforms again into form III, by stretching, and vice versa, when the tension is removed. The relative amount of form III and form II observed in the stress-relaxed fibers depends on the degree of stereoregularity of the sample and on the time the sample is kept under tension.[16] To stabilize the *trans*-planar form III, the fibers have to be kept under tension for a long time. This time increases with decreasing the degree of stereoregularity.

As already known from the literature,[16] stereo- and regioirregular sPP samples, obtained with the vanadium-based Ziegler−Natta catalyst, like for instance the sPP(C) sample, only produce the helical form II by stretching. The X-ray diffraction pattern of a fiber of the sPP(C) sample, stretched at 300% elongation and kept in tension (higher draw ratios would break the sample), is reported in Figure 4. The helical form II is obtained, as indicated by the presence of the equatorial reflections at $2\theta = 12°$ and 17°. The *trans*-planar form III does not form in this low stereoregular sample. The X-ray diffraction pattern of this sample after the release of the tension (not reported) does not show appreciable differences from that one of Figure 4.

The different polymorphic behavior upon stretching shown by the three samples is most likely linked to the different amounts of defects of stereo- and regioregularity of the chains. It has been suggested that defects of stereoregularity and, probably, even regioregularity are highly tolerated within the lattices of the crystalline modifications of sPP with chains in helical conformation,[28] whereas such defects would be hardly included in the crystalline lattice of the *trans*-planar form III. This accounts for our results of Figures 1−4; for the most stereoregular sPP(A) sample the *trans*-planar form III is easily obtained by stretching up to 400% elongation; the less stereoregular sPP(B) sample gives the pure form III only at 600% deformation whereas the most defective sPP(C) sample does not give the pure form III, whatever the draw ratio.

Figure 5 compares the stress−strain curves of the three sPP samples, in the case of the unoriented compression molded specimens (Figure 5a), and for the strained and stress-relaxed fibers (sPP(A′), sPP(B′), and sPP(B″) samples, Figure 5b). The sPP(A′), sPP(B′), and sPP(B″) fibers are obtained by stretching compression-molded sPP(A) and sPP(B) samples up to a given strain

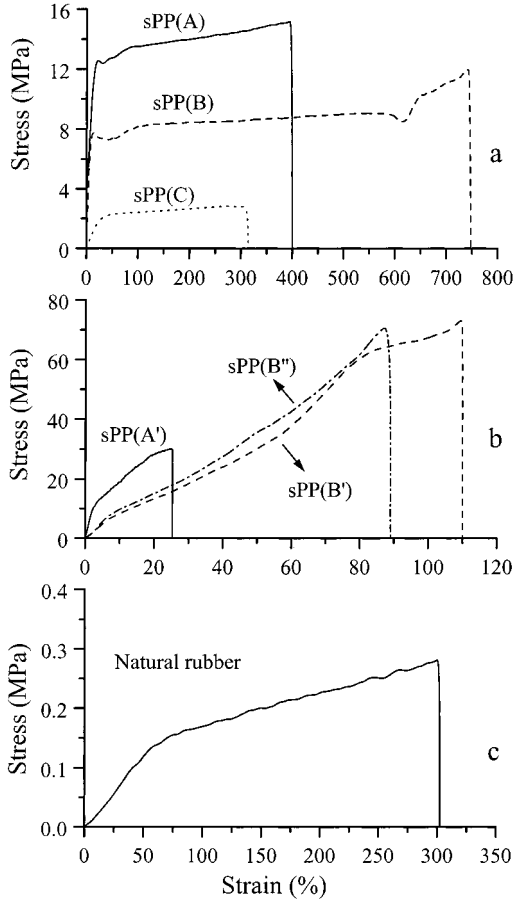

Figure 5. Stress−strain curves recorded at a ratio between the drawing rate and the initial length of the samples equal to 1 mm/(mm min) (initial gauge length 10 mm) for (a) unoriented compression-molded sPP(A) (solid line), sPP(B) (dashed line), and sPP(C) (dotted line) samples; (b) strained and stress-relaxed sPP fibers: sPP(A′) stress-relaxed from sPP(A) sample stretched at 400% elongation (solid line); sPP(B′) stress-relaxed from sPP(B) sample stretched at 400% elongation (dashed line); sPP(B″) stress-relaxed from sPP(B) sample stretched at 600% elongation (dashed−dotted line); and (c) the natural rubber.

ϵ (ϵ = 400% for sPP(A′) and sPP(B′), 600% for sPP(B″)). The fibers are kept in tension for 2 days, and then the stress is removed, allowing the fibers to relax.

The mechanical properties of the samples (i.e., Young's modulus, stress and strain at break, tension set, and elastic recovery at a given elongation) and the degree of crystallinity of the starting unoriented samples (as determined by the X-ray powder diffraction profiles, not shown here) are reported in Table 1. With increasing the amount of defects of stereo- and regioregularity the degree of crystallinity of the starting material decreases; since the rigidity of the materials is mainly an increasing function of the degree of crystallinity, the measured values of the stress for a given strain, the Young's modulus, and the stress at break decrease with decreasing of the degree of crystallinity (see Figure 5a and Table 1). The strain at break of the sPP(B) sample is higher than that of the sPP(A) sample, probably because of its higher polydispersion index. The presence of chains with low molecular mass, acting as plasticizer, probably makes the sample sPP(B) more ductile. The values of the tension set, measured at 400% elongation on specimens not previously oriented, are 300% for the sPP(A) sample and 267% for the sPP(B) sample; the

Table 1. Elastic Modulus (E), Stress (σ_b), and Strain (ϵ_b) at Break, Tension Set ($t_s(\epsilon\%)$), and Elastic Recovery ($r(\epsilon\%)$) at $\epsilon\%$ Deformation and Degree of Crystallinity (x_c) for the Unoriented Compression-Molded and for the Stress-Relaxed SPP Fiber Samples

	E (MPa)	σ_b (MPa)	ϵ_b (%)	$t_s(\epsilon\%)$ (%)	$r(\epsilon\%)$ (%)	x_c (%)
unoriented samples						
sPP(A)	256 ± 20	15 ± 1	400 ± 20	300[a]	25[a]	40
sPP(B)	119 ± 8	12 ± 1	750 ± 20	267[a]	36[a]	30
				333[b]	61[b]	
sPP(C)	17 ± 2	2.8 ± 0.1	300 ± 20	300[c]	0[c]	17
stress-relaxed samples						
sPP(A′)[d]	335 ± 20	30 ± 2	25 ± 5	0[f]	25[f]	
sPP(B′)[d]	128 ± 2	74 ± 2	110 ± 8	4.5[f]	30[f]	
sPP(B″)[e]	167 ± 10	72 ± 2	90 ± 5	4.6[f]	54[f]	

[a] Measured at 400% elongation. [b] Measured at 600% elongation. [c] Measured at 300% elongation. [d] Fibers of the sPP(A) and sPP(B) samples prepared by stretching compression-molded films up to 400% elongation, keeping in tension the fibers for 2 days, and then removing the tension. [e] Fiber of the sPP(B) sample prepared by stretching compression-molded films up to 600% elongation, keeping in tension the fiber for 2 days, and then removing the tension. [f] Measured at 25% (sPP(A′)), 36% (sPP(B′)), and 61% (sPP(B″)) elongation.

latter presents a higher tension set value when measured at a higher draw ratio (t_s = 333% at 600% elongation, i.e., close to the break, see Table 1). The sPP(C) sample basically undergoes a plastic deformation by stretching and does not present any recovery of the initial dimensions upon the release of the tension (t_s measured at 300% elongation is 300%, see Table 1). Therefore, the three samples, when not previously oriented, show only fair or poor elastic properties, regardless of the degree of stereoregularity.

The mechanical properties of the sPP samples change drastically, when measured on previously oriented, stress-relaxed fibers (sPP(A′), sPP(B′), and sPP(B″) samples, Figure 5b): the values of the stress at a given strain are nearly 1 order of magnitude higher than those measured on not previously oriented specimens. Moreover, sPP(A′), sPP(B′), and sPP(B″) fibers show the mechanical properties of a true elastomer almost up to the break (the stress−strain curves are nearly linear), and the values of the tension set are lower than 10% (Table 1). As discussed above, the less stereoregular sPP(C) sample does not present any recovery of the initial dimensions after the plastic deformation, when the tension is removed ($t_s(300\%)$ = 300%, see Table 1). It breaks immediately by further stretching (the stress−strain curve is not reported in Figure 5b).

The stress−strain curve of the sample of natural rubber is reported in Figure 5c for comparison. It is apparent that for the stress-relaxed sPP fibers the values of the stresses, measured at a given deformation, are always higher (of 2 orders of magnitude) than those of the natural rubber.

To obtain more quantitative insight, hysteresis cycles have been performed on the previously oriented stress-relaxed fibers (sPP(A′), sPP(B′), and sPP(B″) samples). Figure 6a,b plots the hysteresis cycles (composed of the stress−strain curves measured during the stretching immediately followed by the curves measured during the relaxing at controlled rate), in the case of the sPP(A′) (solid line), sPP(B′) (dashed line), and sPP(B″) (dashed−dotted line) fibers. More precisely, the sPP(A′), sPP(B′), and sPP(B″) fibers were prepared, as described above, by stretching strips, of initial length L_0, of compression molded samples up to 400% or 600% deformation (the final lengths are $L_f = 5L_0$ for sPP(A′) and sPP(B′) and $L_f = 7L_0$ for sPP(B″)), and then removing the tension; the final length after the relaxation of the fibers is $L_r = [t_s(\epsilon\%)/100]L_0 + L_0$, where the values of the tension set, $t_s(\epsilon\%)$, are 300% and 267% for sPP(A) and sPP(B) relaxed from 400% elongation, respectively, and 333% for sPP(B) relaxed form 600% elongation, see Table 1).

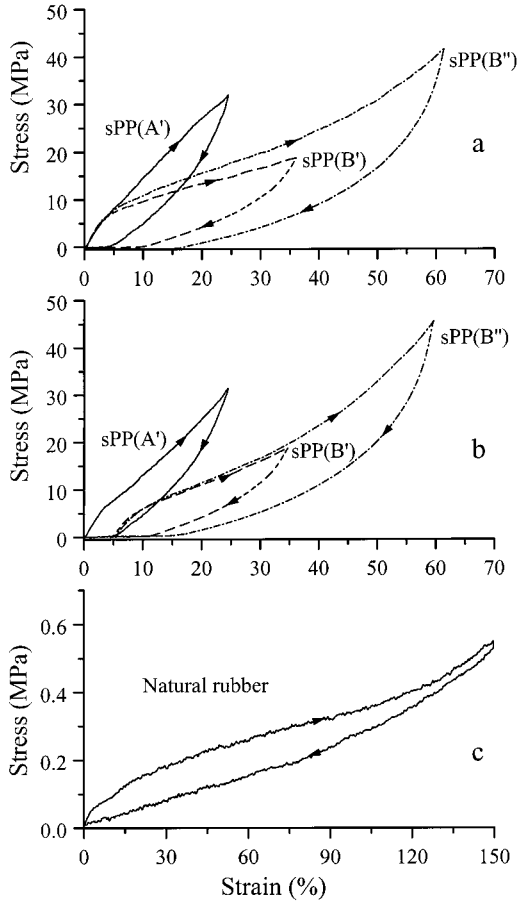

Figure 6. Stress−strain hysteresis cycles, composed of the stretching and the relaxing at controlled rate steps according to the direction of the arrows, for strained and stress-relaxed sPP fibers: sPP(A′) stress-relaxed from sPP(A) sample stretched at 400% elongation (solid line); sPP(B′) stress-relaxed from sPP(B) sample stretched at 400% elongation (dashed line); sPP(B″) stress-relaxed from sPP(B) sample stretched at 600% elongation (dashed−dotted line): (a) first cycle; (b) curves averaged for at least four cycles successive to the first one; (c) stress−strain hysteresis cycle for the natural rubber.

The hysteresis cycles of Figure 6 were measured on the stress-relaxed fibers from the new initial length L_r up to the final length $L_f = 5L_0$ or $7L_0$, that is, up to a maximum strain $\epsilon_{max} = [(L_f - L_r)/L_r] \times 100$, numerically coinciding with the elastic recovery reported in Table 1 (ϵ_{max} = 25% for the sPP(A) sample, stress-relaxed from 400% deformation, 36% and 61% for the sPP(B) samples stress-relaxed from 400% and 600% deformations, respectively). This choice of the maximum strains in the

hysteresis cycles is due to the need to reduce to a minimum a new plastic deformation of the fibers during the first hysteresis cycle.

Figure 6a is relative to the first hysteresis cycle of the stress-relaxed fibers, whereas Figure 6b is relative to the successive hysteresis cycles measured after the first one. Each cycle is performed after 10 min the end of the previous cycle (successive hysteresis cycles measured after the first one are all nearly coincident). The stress-relaxed fibers of the sPP(A) and sPP(B) samples recover almost completely the initial dimensions (tension set values always less than 10%, see Figure 6b), regardless of the initial draw ratio. The energy losses in a hysteresis cycle for the sPP(A′), sPP(B′), and sPP(B″) fibers are 41%, 50%, and 52%, respectively.

The hysteresis curves relative to sample of natural rubber is shown in Figure 6c. In this case much lower values of energy loss in a hysteresis cycle (25%) are involved. (The mechanical energy spent to deform the material during the stretching is almost completely recovered in the successive relaxing step of the hysteresis cycle.)

The deformation behavior of the sPP samples is perfectly reproducible and, for a given sample, depends on the maximum strain ($\epsilon = [(L_f - L_0)/L_0] \times 100$) which the initial unoriented compression-molded strips achieve during the stretching, but not on the number of steps used to achieve the desired deformation. For instance, we have stretched the sPP(B) sample up to 600% deformation in two steps with the following procedure: (a) compression-molded sPP(B) strips were first deformed up to $L_f = 5L_0$ ($\epsilon = 400\%$); (b) the tension is removed, and the final length of the relaxed samples is on average $L_r = 3.67L_0$ (the tension set at 400% elongation being $t_s(400\%) = 267\%$, see Table 1); (c) the samples were stretched again up to $L_f = 7L_0$ ($\epsilon = 600\%$ with respect to the initial length L_0); (d) upon the release of the tension the final length of the relaxed samples was $L_r = 4.33L_0$ and the tension set $t_s(600\%) = 333\%$, which coincides with the value reported in Table 1 and measured on compression-molded strips of the sPP(B) sample deformed up to $L_f = 7L_0$ in a single step.

Fibers of the sPP(B) samples, obtained with the above-described procedure, have shown a mechanical behavior, measured in successive hysteresis cycles, similar to that shown in Figure 6a,b for the sPP(B″) fiber sample, which is stress-relaxed from 600% deformation achieved in a single step.

Despite the relatively high degree of crystallinity of the stress-relaxed sPP(A) and sPP(B) samples, this material shows elastic properties. The comparison between the mechanical analysis (Figures 5 and 6 and Table 1) and the X-ray diffraction patterns (Figures 1−4) indicates that the elastic behavior is possibly due to the reversible crystal−crystal phase transition occurring during the stretching and the releasing of the tension. In fact, the less stereoregular sPP(C) sample, which does not form the *trans*-planar form III and does not show the reversible *trans*-planar helical conformational transition during the stress-relaxing cycles, does not present any elastic behavior.

The comparison with the natural rubber clearly indicates that sPP presents the behavior of a high modulus elastomer thanks to the high crystallinity, the values of the stress necessary to induce a deformation being higher than those of the natural rubber.

Conclusions

The origin of the elastic properties of sPP has been clarified.

As for the most common thermoplastic elastomers, also in the case of sPP the elastic properties originate from a reversible conformational transition. But unlike the most common elastomers, sPP is a highly crystalline material, and the conformational transition occurs in both the crystalline and the amorphous regions. Starting from materials in the stable helical form, a transition from the most stable 2-fold helical $(T_2G_2)_n$ conformation into the less stable *trans*-planar conformation occurs by stretching. The crystalline domains, with chains in helical conformation, tend to assume a preferred orientation along the stretching direction in a not previously oriented material, originating a plastic, not reversible deformation. Along with this plastic deformation, a crystal−crystal phase transition from the most stable crystalline modification with chains in helical conformation into the form III with chains in *trans*-planar conformation gradually occurs. The crystal−crystal phase transition is reversible; after the release of the tension the crystalline domains remain nearly oriented with the *c* axis parallel to the preferred (stretching) direction, and the transition from the metastable *trans*-planar form III into the helical form II occurs. This crystalline transition is the main process involved during the relaxing of the material and is probably mainly responsible for the observed elastic dimensional recovery of the material.

During the transition from the 2-fold helical form into the *trans*-planar form III, an increase of the periodicity per structural unit *h* (which comprises two monomeric units) from $h = c/2 = 3.7$ Å of the 2-fold helical form to $h = c = 5.1$ Å of the *trans*-planar form III is involved. The crystal dimensions increase about 37% along *c*. This increase is completely recovered upon the release of the tension due to the transition of the *trans*-planar form into the helical form, and correspondingly, a reduction of the length of the specimen occurs. As a result, for a not previously oriented material, a partial recovery of the macroscopic dimensions of the sample is attained. (The values of the tension set at elongation close to the break are nearly 300% for both sPP(A) and sPP(B) samples.) The dimensional recovery of previously oriented sPP fibers (like for instance the stress-relaxed sPP(A′), sPP(B′), and sPP(B″) samples examined here) is, instead, nearly total (tension set always <10%), and the material presents very good elastic properties. When the crystalline domains are already oriented along the preferred (stretching) direction, the main process involved during the stretching and relaxing mechanical cycles is the crystal−crystal phase transition. Of course, during the mechanical cycles also the chains in the amorphous regions are subjected to a reversible conformational transition, from the "random coils" into extended conformations, and vice versa. This reversibility of the transition is possibly assisted and is somehow favored by the polymorphic transition occurring in the crystalline regions.

An evidence that the conformational crystal−crystal transition is responsible for the elastic behavior of sPP is provided by the fact that the less stereoregular sPP(C) sample, which does not produce the *trans*-planar form III by stretching, undergoes only plastic, permanent deformations and does not present elastic properties.

In conclusion, while the driving force leading the common elastomers to recover the initial dimensions is mainly entropic, in the case of sPP it is basically linked to the enthalpy gain achieved when the sample is relaxed, a process which involves a crystal−crystal phase transition from the metastable *trans*-planar form III into the more stable helical form II.

It is worth noting that analogous conclusions were drawn in ref 22 in the case of poly(trimethylene terephthalate) (3GT) and poly(tetramethylene terephthalate) (4GT) also showing elastic properties with an associated crystal−crystal phase transition. The diffraction pattern of 3GT changes monotonically with increasing the macroscopic strain, suggesting that the lattice responds immediately to the applied stress and deforms like a coiled spring. In 4GT for low values of the strain the X-ray diffraction pattern does not change; at higher strains changes in the pattern occur, suggesting a definitive change in the crystal structure.[21] In both cases it was concluded that the molecular conformations in both the crystalline and noncrystalline regions play a key role in determining the mechanical behavior of these polymers.[21,22]

Acknowledgment. Financial support of the "Ministero dell'Università e della Ricerca Scientifica e Tecnologica" (PRIN 2000) is gratefully acknowledged.

References and Notes

(1) Holden, G. *Encyclopedia of Polymer Science and Engineering*, 3rd ed.; John Wiley & Sons: New York, 1989.
(2) Natta, G.; Mazzanti, G.; Crespi, G.; Moraglio, G. *Chim. Ind. (Milan)* **1957**, *39*, 275.
(3) Natta, G. U.S. Patent 3,175,999, 1965.
(4) Natta, G. *J. Polym. Sci.* **1959**, *34*, 531.
(5) Collette, J. W.; Tullock, C. W. (Dupont) U.S. Patent 4335225, 1982.
(6) Collette, J. W.; Tullock, C. W.; MacDonald, R. N.; Buck, W. H.; Su, A. C. L.; Harrel, J. R.; Mulhaupt, R.; Anderson, B. C. *Macromolecules* **1989**, *22*, 3851.
(7) Collette, J. W.; Ovenall, D. W.; Buck, W. H.; Ferguson, R. C. *Macromolecules* **1989**, *22*, 3858.
(8) Coates, G.; Waymouth, R. M. *Science* **1995**, *267*, 217.
(9) Hu, Y.; Krejchi, M. T.; Shah, C. D.; Myers, C. L.; Waymouth, R. M. *Macromolecules* **1998**, *31*, 6908.
(10) Mallin, D. T.; Rausch, M. D.; Lin, Y.-G.; Dong, S.; Chien, J. C. W. *J. Am. Chem. Soc.* **1990**, *112*, 2030.
(11) Bravakis, A. M.; Bailey, L. E.; Pigeon, M.; Collins, S. *Macromolecules* **1998**, *31*, 1000.
(12) Dietrich, U.; Hackmann, M.; Rieger, B.; Klinga, M.; Leskelä, M. *J. Am. Chem. Soc.* **1999**, *121*, 4348.
(13) Angeli, D.; Balboni, D.; Baruzzi, G.; Braga, V.; Camurati, I.; Moscardi, G.; Piemontesi, F.; Resconi, L.; Venditto, V.; Antonucci, S. *Macromol. Chem. Phys.* **2001**, *202*, 1780.
(14) Resconi, L.; Jones, R. L.; Rheingold, A.; Yap, G. P. A. *Organometallics* **1996**, *15*, 998.
(15) De Rosa, C.; Corradini, P. *Macromolecules* **1993**, *26*, 5711.
(16) De Rosa, C.; Auriemma, F.; Vinti, V. *Macromolecules* **1998**, *31*, 7430.
(17) Loos, J.; Schimanki, T. *Polym. Eng. Sci.* **2000**, *40*, 567.
(18) D'Aniello, C.; Guadagno, L.; Naddeo, C.; Vittoria, V. *Macromol. Rapid Commun.* **2001**, *22*, 104.
(19) Takahashi, Y.; Sumita, I.; Tadokoro, H. *J. Polym. Sci., Part B* **1973**, *11*, 2113.
(20) Takahashi, Y.; Osaki, Y.; Tadokoro, H. *J. Polym. Sci., Part B* **1981**, *19*, 1153.
(21) Jakeways, R.; Ward, I. M.; Wilding, M. A.; Hall, I. H.; Desborough, I. J.; Pass, M. G. *J. Polym. Sci., Part B* **1975**, *13*, 799.
(22) Ward, I. M.; Wilding, M. A.; Brody, H. *J. Polym. Sci., Part B* **1976**, *14*, 263.
(23) Ewen, J. A.; Jones, R.; Razavi, A.; Ferrara, J. D. *J. Am. Chem. Soc.* **1988**, *110*, 6255.
(24) Natta, G.; Pasquon, I.; Zambelli, A. *J. Am. Chem. Soc.* **1962**, *84*, 1488.
(25) Zambelli, A.; Locatelli, P.; Rovasoli, A.; Ferro, D. R. *Macromolecules* **1980**, *13*, 267.
(26) Ammendola, P.; Shijng, X.; Grassi, A.; Zambelli, A. *Gazz. Chim. Ital.* **1988**, *118*, 769.
(27) Chatani, Y.; Maruyama, H.; Naguchi, K.; Asanuma, T.; Shiomura, T. *J. Polym. Sci., Part C* **1990**, *28*, 393.
(28) Auriemma, F.; De Rosa, C.; Corradini, P. *Macromolecules* **1993**, *26*, 5719.

MA002021J